Low-cost Thin-film Transistor-based Microcantilever for Measuring Deflection

Ping- Yen Lin[*], Yung-Jen Cheng[**], Shu Kuan[***], and Long- Sun Huang[****]

Institute of Applied mechanics, National Taiwan University, Taipei, Taiwan
[*]pylin@mems.iam.ntu.edu.tw , [**]yjcheng@mems.iam.ntu.edu.tw, [***]skuan@mems.iam.ntu.edu.tw
[****]lshuang@mems.iam.ntu.edu.tw

ABSTRATE

This study utilizes thin-film transistor (TFT) as a sensing transducer to convert induced stress of a microcantilever (MCL) into an electric signal. The TFT-based MCL was made by micro-electromechanical system (MEMS) fabrication technology. The mobility of polysilicon TFT fabricated in this work was measured to be 25.11 ± 1.72cm^2/Vs. This study has proven to a significant increase in drain current of released MCLs in comparison with the un-released devices. It was also found that the TFT drain current sensitivity of the chip was measured to be 31nA/μm. We also verified that the reproducible change in drain current confirms the feasibility of TFT-based MCLs for measuring deflection. This study pioneered in design and fabrication of poly-Si TFT onto a suspended MCL. The fabrication incorporated the MOS and POST-MEMS technology, which are both CMOS compatible. As a result, the miniaturized and integrated MCL for bio/chemicalsensors is highly anticipated to be implemented in the future.

Keywords: TFT, microcantilever, MEMS, deflection

1 INTRODUCTION

Microcantilevers (MCLs) appear to be a more promising platform to readily and quantitatively monitor the micromechanical motions [1-3]. Thus, it appears to be more promising platforms for versatile sensors in recent years. The MCL previously applied in atomic force microscopy (AFM) measurement in the late 1980s[4]. As the surface-to-volume ratio increases dramatically with reduced dimensions, surface effects are greatly amplified in the MCL[5] Many researches investigated the effect of the external environment impact on MCL because of the high sensitivity caused by external environment[6-7]. There are several applications based on MCL detection has proposed in recent years. It can be classified as physical measurements and chemical measurement. Aspects in physical measurements, the bending caused by the different coefficient of thermal expansion of composite MCL was used as temperature sensor [1], and the resonance frequency change before and after the analytes binding was used as mass sensor [4]. Aspects in chemical measurements, Baller et al. functionalized a polymer film on MCL to detect surrounding water molecules and other substances [8]. In 1997, Berger et al. successfully detected the binding affinity between self-assembled molecules and gold film coated on MCL [9]. After that, MCLs were served as extremely versatile sensors.

The FET-based stress sensors are widely reported for devices such as accelerometers, resonators, and parallel cantilevers for scanning probe microscopy, as well as for residual stress measurements [10-12]. The stress affects the electronic characteristics, such as the transconductance, of the transistor device.

Recently, the low-cost poly-si thin-film transistors (TFTs) have much higher electron mobility and better reliability. Therefore, polysilicon-based TFT instead of SOI wafer is then used herein. Since the localized stress concentrated on the fixed side of MCL, the embedded TFT would witness the local strain caused by applied stress. In this work, the TFT-based MCL which we fabricated and the conversion mechanism by induced surface stress as shown in figure 1. The external strain was applied to a free end of MCLs using a micropositioner in a desired step size ranging from 0 to 25μm. The strain effect in N-channel as a function of bending was investigated by electrical behavior. When strain is applied, the channel of transistor distorts that induce band gap splitting and occurrence in defects, thus the mobility of transistor change. Then the output response of drain current will change.

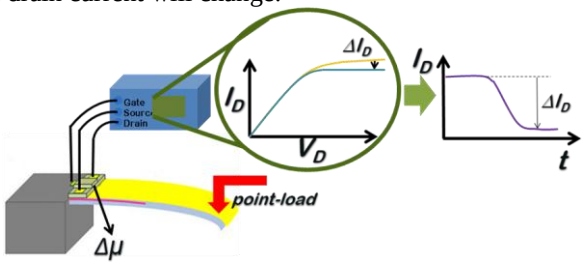

Figure 1. The schematic of the principle of TFT-based MCL operation

2 MATERIALS AND METHODS

The design of TFT-embedded MCL classified TFT design and MCL design. Both TFT and MCL need to match each other, so the TFT use sentaurus TCAD to simulate the electrical performance of TFT before stress applied by different conditions, and the MCL needed to design according to the parameters of film's materials. Then, the optimal parameters could be used in fabrication process.

2.1 TFT design and simulation

In TFT design, the channel material, doping type, doping concentrations, width/length ratio were the main factors need to consider.

The poly-Si was chose to be the channel material because the high mobility than a-Si. The source and drain were implanted the phosphorus as n-type transistor. The concentration which computed by doping profile is $2E19\,cm^{-3}$, energy is 27keV. The drain current will be affected by the channel width and length ratio(W/L ratio). The W/L ratio will be restricted by the MCL size, so we chose channel width and length both were 70μm and 10μm. we used Sentaurus TCAD to estimate the performance according to the conditions previously described. The drains current are 14μA and 6μA at the V_G are 8V and 6V respectively.

2.2 Residual stress match

The MCL design needed to take the film thickness, the position and the direction of transistors into account. The neutral axis and the residual stress are the main factors. In the neutral axis, there is no strain changed, so it noted that the channel needed to away from the neutral axis. The residual stress is the main factor which causes the MCL bending after releasing. It is needed to take the residual stress, thickness of each layer into account. The maximum stress concentrated on the fixed end of the MCL[13], so TFT needed to set in the fixed end. The direction of TFT which we set in the MCL classified into two types, transverse and longitudinal. Finally, we expect that the initial curvature of MCL after releasing is straight (not curved up) which can present the large sensing windows for detection.

The TFT is back-gate type because the channel would be far from neutral axis, and the gate layer is poly-Si, the dielectric layer is SiO_2, the channel is poly-Si, the top and bottom layers of TFT were Si_2N_3 as the passivation and MCL structure. The length and width of beam are 200μm and 150μm respectively.

2.3 Measurement conditions

All devices measured by Agilent 4156C precision semiconductor parameter analyzer, and the external load was applied to a free end of MCLs using a micropositioner in a desired step size ranging from 0 to 25μm. The channel would be compressed or tensile when the MCL bending. The electric performance of TFT-embedded MCL would be dramatically changed.

There are transverse and longitudinal two types of TFT-embedded MCL. Both were measured in the same conditions. Firstly, each device measured before Si_2N_3 deposited, the result can previously test whether it could work or not, and compare with simulations. Then, the change of output signal after MCL bends is measured from I_D change of I_D-V_D chart. The Vg used in the experiments is from 5~7V. As Vg over 8V the leakage current becomes very large, thus the TFT characteristic (saturation current) no longer exists. It notes that the MCL needs to be controlled in the TFT working zone.

3 FABRICAITON PROCESS FLOW

The fabrication was performed by a standard CMOS and post-CMOS MEMS process to release MCL. The process flow is described as show in figure 2. First, the nitride was deposited on the p-type silicon wafer as main structure of MCL. Then, the un-doped 100nm-thick poly-Si was deposited by LPCVD on the nitride as gate layer, and the phosphorus is implanted as poly gate. Then, the 50nm-thick oxide was deposited by furnace on the poly-Si as gate oxide, and the 100nm-thick poly-Si was continuously deposited by LPCVD on the gate oxide as active layer, and the e phosphorus was implanted to define source/drain region. These dopants were activated by rapid thermal annealing. Then, the active region was defined by RIE dry etching. After that, the 250nm-thick metal layer was deposited and then patterned for the source/drain and gate region as the metal pad. Afterward, the 250nm-thick nitride was deposited by PECVD as the passivation. Next the MCL was defined by RIE dry etching. Finally, the MCL was released by KOH backside etching.

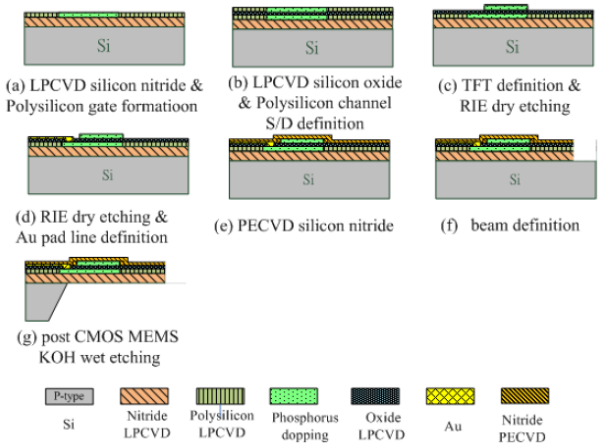

Figure 2. process flow for TFT-based MCL

4 EXPERIMENTAL RESULTS

The experiments included the different TFT electric characteristics before and after releasing, and the relationship between transistor and the deflection of MCL, and compare the change of different channel types with the bending. Figure 3 showed the SEM picture of sensor chip.

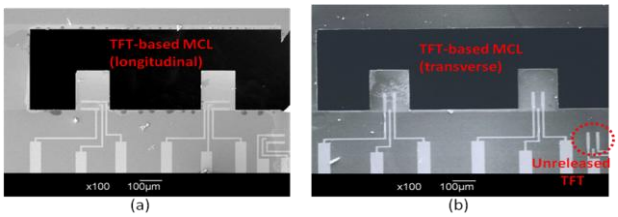

Figure 3. SEM image showing the stress match. (a) the longitudinal TFT (b) the transversal TFT

4.1 Id-Vd of embedded vs. unreleased and released TFT

Figure 4 showed the comparison among the TFT before and after depositing the Si_2N_3, TFT-embedded MCL before and after releasing. Firstly, we found the Si_2N_3 capping layer used for top passivation and TFT-embedded MCL after releasing can let the drive current dramatically enhanced up to3.6 and 3.8 fold respectively. Secondly, the change of drive current before and after releasing is minor about 6%. That means the residual stress of materials is the major effect in enhancing the TFT electric performance.

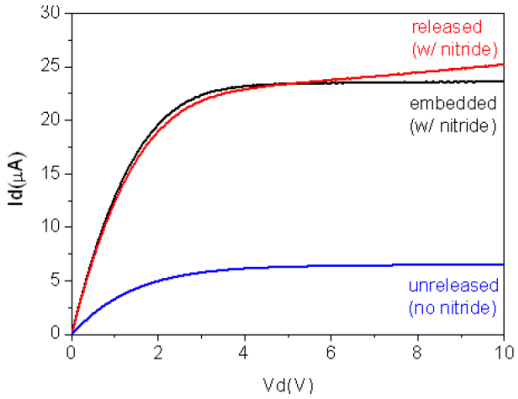

Figure 4. The comparisions of SiN capping effect to electrical characteristics $I_D(V_{DS})$ between bare , unreleased and released TFT.

4.2 I_D-V_D change with deflection by the point-load

The TFT-embedded MCL was bend by the probe, the probe applied deflections is gradually increasing from 0 to 25μm.

Figure 5 shows the relationship between I_D-V_D and deflection. The I_D reduced when applying point-load, and the I_D change would be larger as the V_G increasing. Because of the maximum change of I_D, the optimal operating condition is V_G=7V.

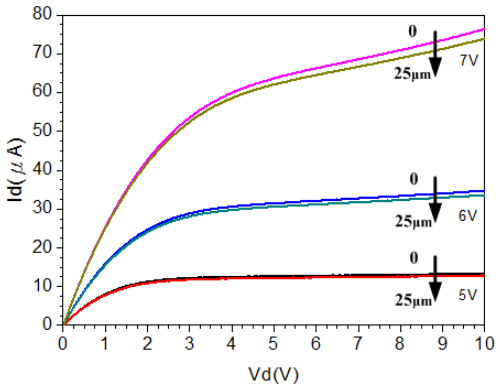

Figure 5. The comparison before and after the MCL bending from V_G=5V to 7V

4.3 I_D change in transverse and longitudinal TFT

Figure 6(a) indicated the force sensitivity of longitudinal TFT, the V_G operate above the Vth from 5V to 7V, the force sensitivity increased as the V_G rising. Figure 6(b) show the force sensitivity of transverse TFT, and the trend is the same with the longitudinal TFT. We could find there is a maximum sensitivity when V_G is 7V at transverse TFT. It is also implied the optimal operating conditions when the device is used on biomedical applications.

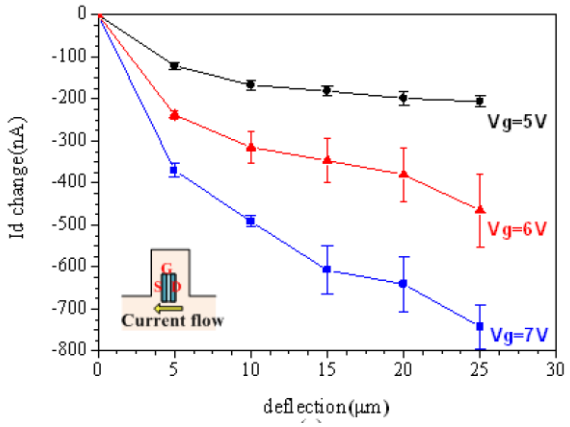

(a)

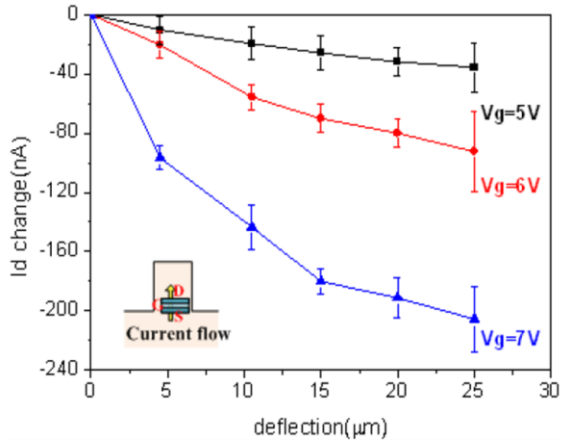

(b)

Figure 6. change in drina current of embedded TFT as a result of MCL bending (a) transversal TFT (b) logitudinal TFT

4.4 Initial drive current vs. sensitivity

Figure 7 indicated the relationship between sensitivity and saturation drain current($I_{D,sat}$) with no strain applied, the trends implied that the sensitivity and $I_{D,sat}$ has the linear relationship, and the slope in different V_G is substantially different. The slop are 0.9 mm^{-1}, 0.6 mm^{-1} and 0.5 mm^{-1}as V_G=5V, 6V and 7V respectively. It also showed the

NSTI-Nanotech 2011, www.nsti.org, ISBN 978-1-4398-7139-3 Vol. 2, 2011

verification of reproducible change in drain current confirms the feasibility of TFT-based MCLs for measuring deflection. It also showed that higher $I_{D,sat}$ will cause the higher sensitivity.

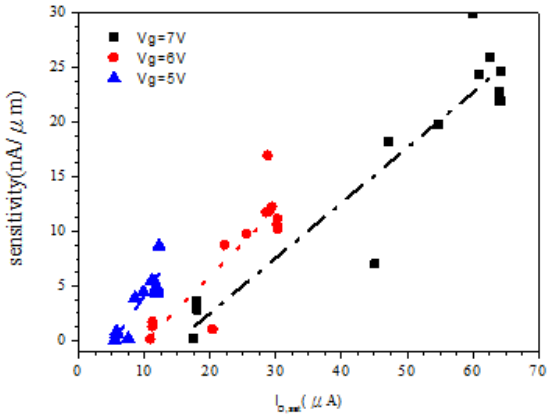

Figure 7. The sensitivity and $I_{D,sat}$ distribition in transversal TFT from V_G=5V to 7V

5 CONCLUSION

This study successfully used MEMS process technology to fabricate the sensors of TFT-based MCL which converted induced stress of MCL into an electrical signal. The initial curvature of MCL after releasing is straight (not curved up) which can present the large sensing windows for detection. The slightly drain current change before and after releasing could attribute to the initial bending of MCL, it caused by the induced residual stress after releasing. The mobility of TFT-embedded MCL after releasing was 25.11± 1.72 cm^2/Vs. The maximum sensitivity measured on wafer by pressing the probe gradually from 0 to 25μm is 31nA/μm. The sensitivity and $I_{D,sat}$ has the linear relationship, so it is possible to increase the sensitivity by enhancing the mobility. This study verified that the reproducible change in drain current confirms the feasibility of TFT-based MCLs for measuring deflection.

The TFT-based MCLs replaced the high cost SOI-based MOSFET by thin film transistors. The cost is lower than SOI MOSFET-based MCL, so it has the potential for point-of-care personalized diagnosis and parallelization for high-throughput screening. Further improvements will carry on enhancing poly-Si grain size for high sensitivity.

REFERENCES

[1] Ziegler, C. (2004). "Cantilever-based biosensors." *Analytical and Bioanalytical Chemistry* **379**(7): 946-959.

[2] Meyer, G. and Amer, N. M. (1988). "Novel optical approach to atomic force microscopy." *Applied Physics Letters* **53**(12): 1045-1047.

[3] Napoli, M., Bamieh, B. and Turner, K. (2004). "A capacitive microcantilever: Modelling, validation, and estimation using current measurements." *Journal of Dynamic Systems Measurement and Control - Transactions of the Asme* **126**(2): 319-326.

[4] Binnig, G., Quate, C. F. and Gerber, C. (1986). "Atomic Force Microscope." *Physical Review Letters* **56**(9): 930.

[5] Pramanik, C., Saha, H. and Gangopadhyay, U. (2006). "Design optimization of a high performance silicon MEMS piezoresistive pressure sensor for biomedical applications." *Journal of Micromechanics and Microengineering* **16**(10): 2060-2066

[6] Thundat, T., Warmack, R. J., Chen, G. Y. and Allison, D. P. (1994). "Thermal and ambient-induced deflections of scanning force microscope cantilevers." *Applied Physics Letters* **64**(21): 2894-2896.

[7] Barnes, J. R., Stephenson, R. J., Welland, M. E., Gerber, C. and Gimzewski, J. K. (1994). "Photothermal spectroscopy with femtojoule sensitivity using a micromechanical device." *Nature* **372**(6501): 79-81.

[8] Baller, M. K., Lang, H. P., Fritz, J., Gerber, C., Gimzewski, J. K., Drechsler, U., Rothuizen, H., Despont, M., Vettiger, P., Battiston, F. M., Ramseyer, J. P., Fornaro, P., Meyer, E. and Guntherodt, H. J. (2000). "A cantilever array-based artificial nose." *Ultramicroscopy* **82**(1-4): 1-9.

[9] Berger, R., Delamarche, E., Lang, H. P., Gerber, C., Gimzewski, J. K., Meyer, E. and Guntherodt, H.-J. (1997). "Surface Stress in the Self-Assembly of Alkanethiols on Gold." *Science* **276**(5321): 2021-2024.

[10]Hamada, A., Furusawa, T., Saito, N., and Takeda, E., "A New Aspect of Mechanical Stress Effects in Scaled MOS Devices", *IEEE Trans Electron Devices*, 38, Apr. 1991, pp. 895-890.

[11] Jaeger, R. C., Suhling, J. C., Ramani, R., Bradley, A. T., and Xu, J. P., "CMOS Stress Sensors on (100) Silicon", *IEEE J. Solid-State Circuits*, 35, Jan. 2000, pp. 85-95.

[12].Koganemaru, M., Ikeda, T., Miyazaki, N., Tomokage, H., 2010. Experimental Study of Uniaxial-Stress Effects on DC Characteristics of nMOSFETs. *Ieee Transactions on Components and Packaging Technologies* 33(2), 278-286.

[13] Goericke, F. T. and King, W. P. (2008). "Modeling Piezoresistive Microcantilever Sensor Response to Surface Stress for biochemical Sensors." *Sensors Journal, IEEE* 8(8): 1404-1410.